Potential and Probability of Inner Ear Magnetic Resonance Imaging at 7 T

Kyoung-Nam Kim[1], Gyu Cheol Han[2], Phil Heo[1], Hongbae Jeong[1], Suk-Min Hong[1], Joshua Haekyun Park[1], Myung-Kyun Woo[1], Young-Bo Kim[1], and Zang-Hee Cho[1]
[1]Neuroscience Research Institute, Gachon University, Incheon, Korea, [2]Department of Otolaryngology-HNS, Gachon University, Incheon, Korea

INTRODUCTION

The cochlear and the vestibular system play important roles in sound perception and maintaining the body equilibrium by sensing body movements and sending signals to the brain through mechano-electric transduction. In order to use MRI for diagnosing inner ear diseases, improvement in the image sensitivity of MR and the development of an optimized RF coil and proper sequence protocol are needed. The switch to ultra-high field (UHF, $\geq$ 7 Tesla) in vivo MRI is promising method due to the high signal intensity (SI). However, despite the benefit of the increased SI of the UHF MR scanner, problems remain, such as the inhomogeneous distribution of the magnetic field, limited penetration depth, and increasing temperature in biological tissue of the human body [1, 2]. In this study, an inner ear RF coil based on multiple smaller element coil arrays was developed allowing inner ear MR imaging with high SI and high spatial resolution at 7 T. We presented preliminary results for visualization of the inner ear using a customized RF coil and without the use of a contrast medium.

MATERIALS AND METHODS

The inner ear MR image using a customized RF coil (Fig. 1) was implemented in the 7 T scanner (Magnetom, Siemens Healthcare, Erlangen, Germany). A single element coil in the RF coil arrays (Fig. 1b) was 5 cm × 5 cm. The gaps between each single element were set at 0.6 cm intervals to decrease the mutual inductance coupling between coil elements. Phantom studies were conducted using a spherical phantom (Siemens, Part Number; 10496809 K2305) and the following acquisition gradient echo (GE) imaging parameters (TR = 400 ms, TE = 10 ms, α = 30°, FOV = 256 × 256 mm, acquisition time = 1 min 42 s) in the transverse orientation. The acquired MR images for the two RF coils, namely a conventional birdcage (BC) coil and dual RF coil arrays, were compared using the one-dimensional (1-D) signal intensity (SI) profile and then the optimal coil configuration for inner ear imaging was compared and selected. For the in vivo inner ear imaging of a healthy volunteer, various pathology using a T_1-weighted volumetric interpolated breath-hold examination (VIBE) imaging [3] sequences (TR = 30 ms, TE = 2.78 ms, α = 6°, FOV = 200 × 200 mm, voxel size = 0.4 × 0.4 × 0.4 mm^3, slice thickness = 0.45 mm, bandwidth = 200 Hz, acquisition time = 5 min 41 s) were utilized with dual RF coil arrays.

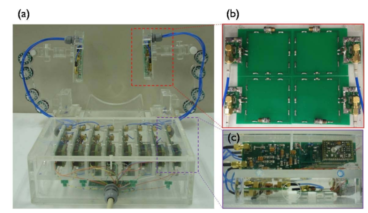

Fig 1: The (a) customized RF coil array consists of (b) dual four element RF coil arrays and (c) their RF circuitry.

RESULTS

The 1-D SI profiles according to GE images for two RF coils were acquired and compared using a spherical phantom and identical imaging parameters (bottom of Fig. 2). Each MR image created by the sum-of-squares (SOS) algorithm was rescaled by a factor of 10 due to the saturated MR signal. The SI of the RF coil arrays corresponds to the characteristics of the surface RF coil and shows a rapid decrease from near the RF coil plane toward the outside of the phantom [4]. The RF coil arrays have significantly higher SI than the commercial BC coil in the peripheral regions such as ROI1 and ROI3, which indicate practical imaging regions between the end of the spherical phantom and approximately 5 cm away from it. In healthy volunteer studies, the 3-D high-resolution MR images were derived from the 2-D inner ear image through the VIBE imaging sequence. The in vivo normal anatomy image of the membranous labyrinth was obtained with the RF coil arrays. The 7 T image reveals the detailed structure of the entire inner ear cochlear and clearly depicts the three semicircular canals with vestibulo-cochlear nerve of a single healthy volunteer. Visualization of the inner ear was also demonstrated (Fig. 3). Note that 7 T inner ear images show high SI for specific membranous organs or nervous tissue such as the clearly separated membranous portion of cochlear and three semi-circular canals, sharp edge of ductus reunions, ampullary nerve, clearly defined facial nerve, vestibluo-cochlear nerve and it allows adequate inspection of the surrounding fine anatomy.

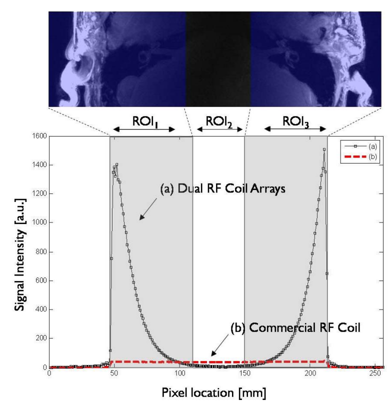

Fig 2: 2-D inner ear VIBE images from a healthy volunteer (upper part) and signal intensity profiles from a spherical phantom (bottom part). Signal intensity profiles for (a) RF coil arrays and (b) commercial RF BC volume coil through transverse slices passing approximately through the center of the spherical phantom.

CONCLUSION AND DISCUSSION

The preliminary results for visualization of the inner ear were based on the technical evaluation of the RF coil arrays and VIBE sequence and were employed at 7 T. Imaging tools using the VIBE sequence provide inner ear images with high spatial resolution and provide useful pathological information. The high-resolution imaging at 7 T appears to be a feasible tool to accurately discern structural anatomy. Effective implementation of customized RF coil technology and spatial imaging protocols that enable acquisition of high spatial resolution images are potentially useful for investigating morphological changes in the inner ear.

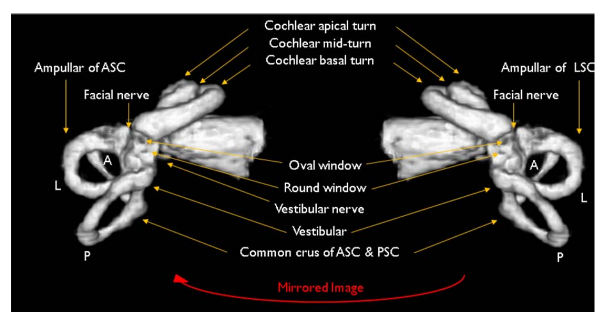

Fig 3: Normal anatomy of the left side membranous labyrinthine was obtained by the three-dimensional VIBE protocol at 7 T (superior and inferior view of the left ear). ASC: anterior semicircular canal; LSC: lateral semicircular canal; PSC: posterior semicircular canal.

REFERENCES

[1] Yang QX et al, Magn Reson Med 2004;52:1016-1020 [2] Collins CM et al, Magn Reson Med 1998;40:847-856 [3] Takahashi N et al, ISMRM 2001 [4] McRobbie DW et al, Cambridge university press, pp182, 2003.

ACKNOWLEDGEMENTS

This work was supported by a Korea Science and Engineering Foundation (KOSEF) grant funded by the Korean Government (Grant no. 20100002134).